The Iceland-Faroe Slope Jet: A conduit for dense water toward the Faroe Bank Channel overflow

Stefanie Semper*[1], Robert S. Pickart[2], Kjetil Våge[1], Karin Margretha Húsgarð Larsen[3], Hjálmar Hátún[3], and Bogi Hansen[3]

1 – Geophysical Institute, University of Bergen and Bjerknes Centre for Climate Research, Bergen, Norway.

2 – Woods Hole Oceanographic Institution, Woods Hole, Massachusetts, USA.

3 – Faroe Marine Research Institute, Tórshavn, Faroe Islands.

* *Corresponding author address:* Geophysical Institute, University of Bergen and Bjerknes Centre for Climate Research, Allégaten 70, 5007 Bergen, Norway.

E-mail: stefanie.semper@uib.no

Dense water from the Nordic Seas passes through the Faroe Bank Channel and supplies the lower limb of the Atlantic Meridional Overturning Circulation (AMOC), a critical component of the global climate system, yet the upstream pathways of this dense water are not fully known. Here we present evidence of a deep current following the continental slope from Iceland toward the Faroe Bank Channel, using high-resolution observations of temperature, salinity, and velocity from a shipboard survey in 2011 along with long-term water column measurements north of the Faroe Islands. The bulk of the volume transport of this current, hereafter referred to as the Iceland-Faroe Slope Jet (IFSJ), is relatively uniform in temperature and salinity. The hydrographic properties of the North Icelandic Jet flowing westward toward Denmark Strait are very similar, which suggests a common source for both of the two major dense overflows across the Greenland-Scotland Ridge. We estimate that the IFSJ accounts for approximately half of the total overflow transport through the Faroe Bank Channel. As such, it is a significant component of the overturning circulation in the Nordic Seas, the main source region of dense water to the AMOC.

The Nordic Seas, comprising the Norwegian, Greenland, and Iceland Seas, are a critical region at the northern extremity of the Atlantic Meridional Overturning Circulation (AMOC). Warm and saline Atlantic Water flowing northward across the Greenland-Scotland Ridge releases heat to the atmosphere and helps maintain the temperate climate of northwest Europe[1;2]. The resulting cold, dense water returns southward at depth as overflow plumes through gaps in the ridge (Fig. 1a). The dense water masses which constitute the overflows (defined as $\sigma_\Theta \geq 27.8\,\mathrm{kg\,m^{-3}}$, hereafter referred to as overflow water[3]) are formed both within the boundary current system around the Nordic Seas and in the interior basins of the Greenland and Iceland Seas. The former product is referred to as Atlantic-origin water, while that formed in the interior, which is the densest contributor to the lower limb of the AMOC, is referred to as Arctic-origin water[4;5]. Recent studies have focused primarily on Denmark Strait between Greenland and Iceland, which is the second-deepest passage (approximately 650 m) through the ridge and has the largest volume transport of overflow water[6–10]. The Atlantic-origin overflow in Denmark Strait is supplied by two branches of the East Greenland Current[6;11], while the Arctic-origin overflow is advected by the North Icelandic Jet (NIJ)[5;6;12] originating northeast of Iceland[5;13].

The densest Arctic-origin overflow water emanating from the Nordic Seas passes through the approximately 850 m deep Faroe Bank Channel (FBC)[10;14] and is subject to extensive mixing and entrainment south of the Greenland-Scotland Ridge[15–17]. The magnitude of the FBC overflow has been monitored continuously since 1995; the most recent estimate of its volume transport is $1.9 \pm 0.3\,\mathrm{Sv}$[10;18] ($1\,\mathrm{Sv} \equiv 10^6\,\mathrm{m^3\,s^{-1}}$). The bulk of this transport is composed of intermediate and deep water masses[14;16]. The former is most likely ventilated during winter in the Iceland and Greenland Seas, with a contribution from the Arctic Ocean[15;19]. The precise origin of the latter water mass remains uncertain.

Before reaching the sill in the FBC, the overflow waters pass through the Faroe Shetland Channel (Fig. 1a). While the hydrographic properties of the water masses in the channel and their interannual variability are well documented[10;18;20], the dense-water pathways feeding this passage are as of yet not fully determined. Here we provide evidence of a deep current following the northern slope of the Greenland-Scotland Ridge from Iceland toward the Faroe Islands. This bottom-intensified current, which we refer to as the Iceland-Faroe Slope Jet (IFSJ), transports water matching the densest water observed in the FBC and may supply approximately half of the total FBC overflow. As such, the IFSJ constitutes a significant component of the overturning in the Nordic Seas, a region which is of key importance to the AMOC[21;22]. To predict the AMOC's response to a changing climate, it is imperative to know the origin and pathways of the dense water supplying its lower limb.

Pathway and transport of the IFSJ

Using high-resolution hydrographic/velocity measurements from a September 2011 shipboard survey (Fig. 1b), we identified a spatially coherent eastward flow between northeast Iceland and the Faroe Islands. Vertical sections of absolutely referenced geostrophic velocity (Fig. 2), which were constructed from the combined hydrographic and velocity fields (see the methods section for details), show that the IFSJ has a consistent hydrographic and kinematic structure. The narrow current is bottom-intensified and comprises two cores of overflow water, which approximately follow the 750 and 1100 m isobaths, respectively. It is composed of cold, dense water that is banked up against the slope (supplementary information, Figs. S1 and S2). An extensive collection of hydrographic measurements from the Nordic Seas[23;24] confirms the persistent presence of anomalously dense water on the upper slope north of Iceland and the Iceland-Faroe Ridge. This isopycnal structure supports the bottom-intensified IFSJ flowing eastward toward the FBC. It is also consistent with the NIJ flowing westward toward Denmark Strait, which is middepth-intensified as the isopycnal tilt reverses again in the upper part of the water column[5;13]. East of the Kolbeinsey Ridge, the extension of the mid-Atlantic Ridge north of Iceland, the two currents are in close proximity (Fig. 1a). While it is well documented that the NIJ emerges northeast of Iceland[5;13], the origin of the IFSJ remains unknown. Recent work suggests that both currents are supplied by dense water emanating from the Greenland Sea gyre that subsequently flows southward through the Iceland Sea along the Kolbeinsey Ridge[24]. Eastward flow of dense water through the Spar Fracture Zone may also supply the IFSJ (Fig. 1b).

The mean volume transport of overflow water in the IFSJ, estimated from the high-resolution hydrographic/velocity sections, is 1.0 ± 0.1 Sv (Fig. 3a). While this value stems from only one survey, the results suggest that the IFSJ may supply approximately half of the total overflow through the FBC (1.9 ± 0.3 Sv)[10;18]. On two sections (B and C) the deep core was not completely bracketed by the observations, resulting in an underestimated transport. The increase in transport between sections C and D may additionally be caused by entrainment of ambient

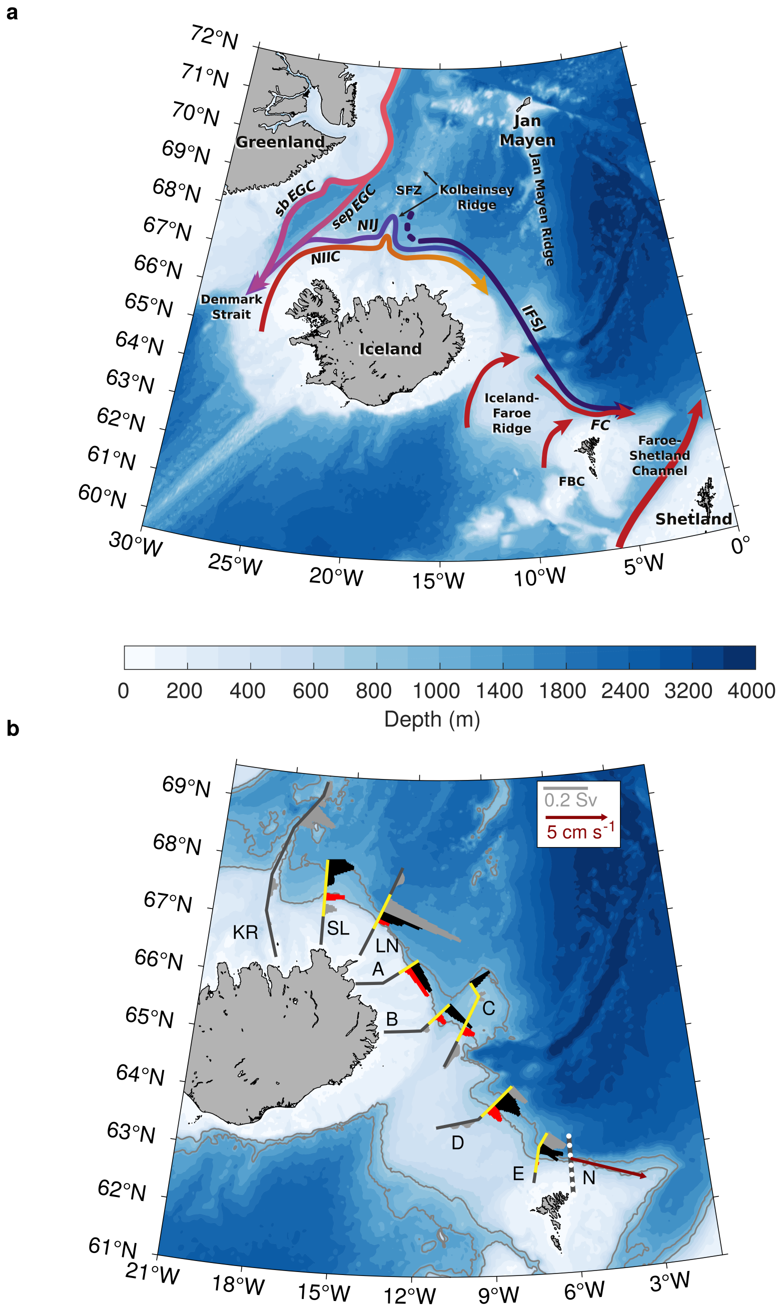

Figure 1: Bathmetry and circulation near the Greenland-Scotland Ridge. a) Schematic pathways of the inflow of Atlantic Water (red arrows) and the outflow of dense water (purple arrows). The acronyms are: FC = Faroe Current; NIIC = North Icelandic Irminger Current; sb EGC = shelfbreak East Greenland Current; sep EGC = separated East Greenland Current; NIJ = North Icelandic Jet; IFSJ = Iceland-Faroe Slope Jet; FBC = Faroe Bank Channel; SFZ = Spar Fracture Zone. b) Transport of overflow water ($\sigma_\Theta \geq 27.8\,\mathrm{kg\,m^{-3}}$) across the high-resolution shipboard transects used in the study. The shallow and deep IFSJ cores are marked in red and black, respectively, and the remaining transport is marked in grey. The segments of the transects shown in Fig. 2 are highlighted in yellow. The three westernmost transect names are abbreviated as: KR = Kolbeinsey Ridge, SL = Slétta, and LN = Langanes Northeast. The mean velocity in the strongest part of the IFSJ from the year-long offshore mooring record at section N is shown in dark red. The stations at section N are indicated by white dots. The colored shading in a) and b) is the bathymetry from ETOPO1[25]; the 750 and 1100 m isobaths are highlighted in grey.

water from the Norwegian Basin, while the low transport at section E likely results from a mesoscale feature suppressing the $27.8\,\mathrm{kg\,m^{-3}}$ isopycnal (Fig. 2). The volume transport was conservatively estimated only for depths shallower than 850 m, the approximate depth of the FBC sill. However, water may be lifted from greater depths by aspiration and supply the overflow[26]. If the depth restriction is removed, the total contribution of the IFSJ to the FBC overflow, according to the 2011 shipboard survey, could be as high as $1.4 \pm 0.2\,\mathrm{Sv}$ (Fig. 3a).

The bulk of the IFSJ's volume transport is confined to a small range in Θ-S space (Fig. 3b). The locus of the Θ-S classes with the highest transport, which we refer to as the transport mode, is centred near $-0.52 \pm 0.11\,^{\circ}\mathrm{C}$ and $35.075 \pm 0.003\,\mathrm{g\,kg^{-1}}$ in temperature and salinity, respectively. While the upper part of the IFSJ becomes warmer and more saline as it progresses eastward, due to mixing with Atlantic Water near the Faroe Islands, the hydrographic properties of the transport mode are not significantly modified along the current's pathway. The density of the transport mode is $\sigma_\Theta = 28.06\,\mathrm{kg\,m^{-3}}$. This is not significantly denser than the transport mode of the NIJ ($\sigma_\Theta = 28.05\,\mathrm{kg\,m^{-3}}$), which has a higher temperature ($-0.29 \pm 0.16\,^{\circ}\mathrm{C}$) but the same salinity[13]. The similarity of these transport modes suggests that the water masses in the two currents have the same origin. Waters of sufficient density are regularly ventilated in the Greenland Sea during winter[27], and their hydrographic properties closely match the two modes[24]. As such, this water mass supplies the densest portions of the two major overflows across the Greenland-Scotland Ridge, and changes in dense water formation in the Greenland Sea may affect both pathways.

As with the IFSJ, the NIJ is often composed of separate cores[13]. In particular, northeast of Iceland the slightly warmer NIJ flows toward Denmark Strait along the 600 and 800 m isobaths, while the slightly colder IFSJ flows toward the FBC approximately along the 750 and 1100 m isobaths. Notably, the 600 and 750 m isobaths are comparable to the sill depths of Denmark Strait and the FBC, respectively. This implies that hydraulic control occurring at the two passages[26;28;29] may be influencing the shallow core of each current.

Data from past studies have hinted at a deep flow along the northern side of the Iceland-Faroe Ridge. Four moorings deployed during 1988–1989 along the 1000 m isobath recorded a deep, bottom-intensified current with temperatures and densities corresponding to the transport mode of the IFSJ[30]. This pathway was also identified in a two-layer numerical model with realistic bathymetry[31]. Furthermore, a subset of

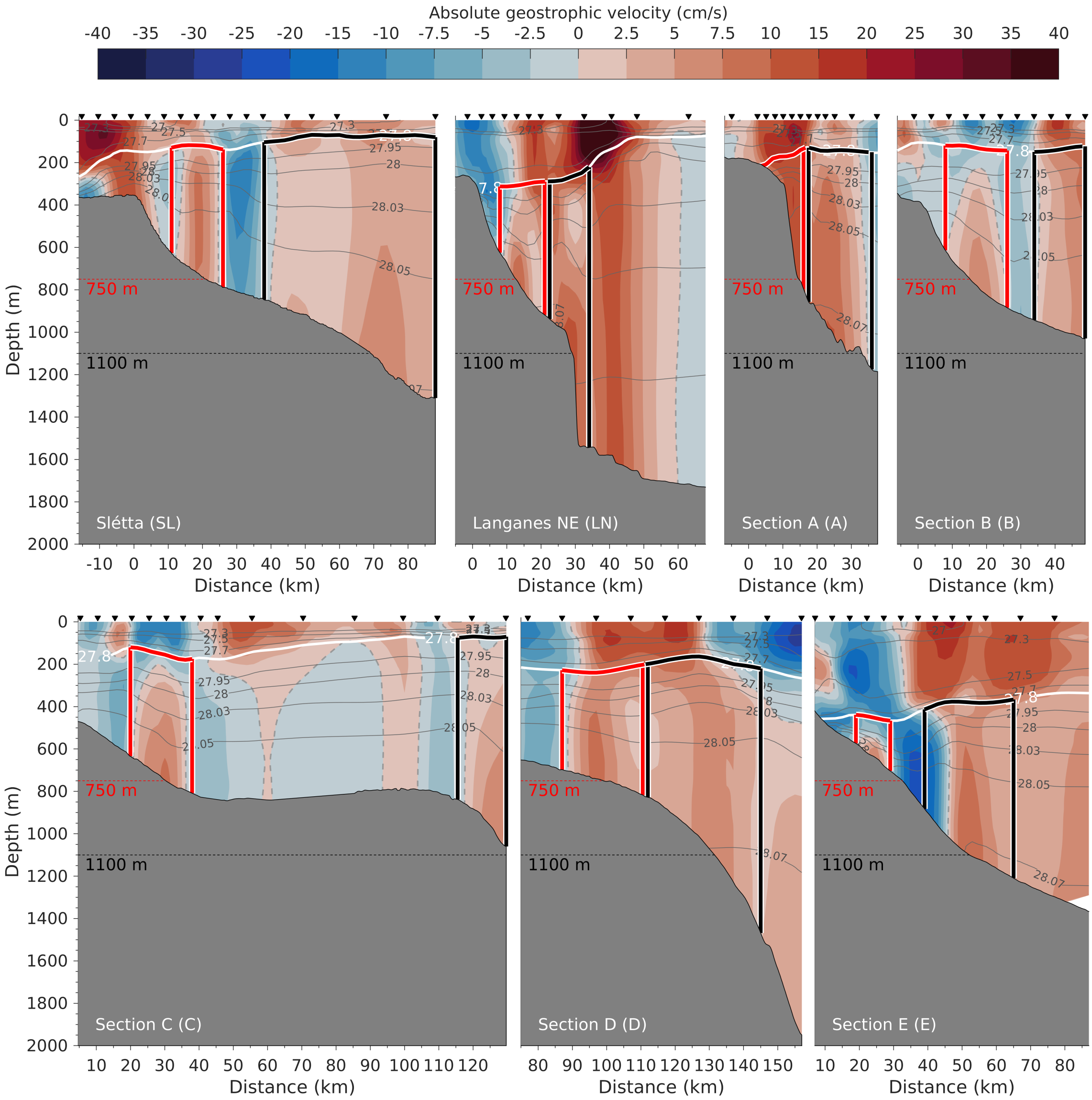

Figure 2: Vertical sections of velocity across the IFSJ. Absolutely referenced geostrophic velocity (colour) and density (thin grey lines) for the yellow segments of the shipboard transects in Fig. 1b. The thick white line is the $27.8\,\mathrm{kg\,m^{-3}}$ isopycnal. The black inverted triangles indicate the locations of the hydrographic profiles. For each transect the origin (distance $y = 0\,\mathrm{km}$) was placed at the shelf break (for sections north of Iceland) or the point where the slope gradient starts to increase (for sections north of the Iceland-Faroe Slope). Positive velocities are directed toward the Faroe Islands. The red and black boxes outline the shallow and deep cores, respectively. The abbreviated names in parentheses are used as labels in Fig. 1. The bathymetry is from the ship's echosounder.

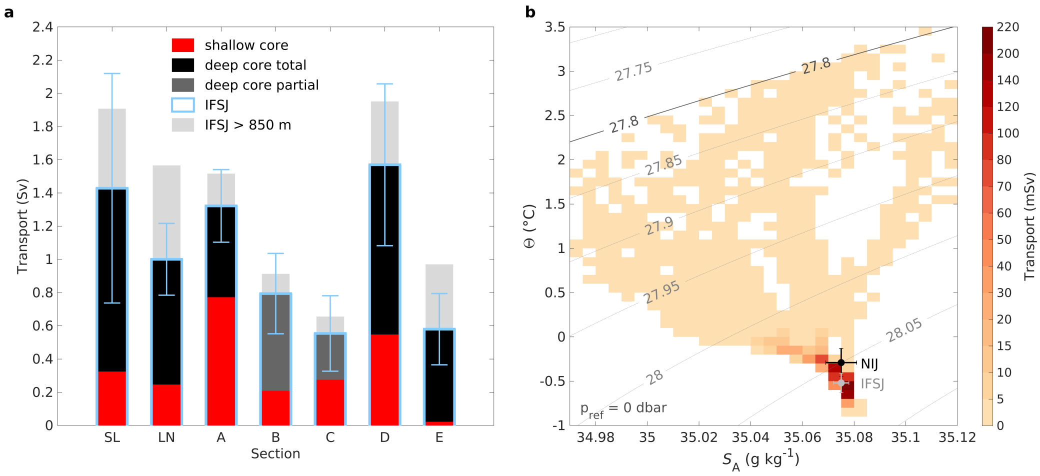

Figure 3: Transport of overflow water ($\sigma_\Theta \geq 27.8\,\mathrm{kg\,m^{-3}}$) in the IFSJ. a) Volume transport for each transect of the high-resolution shipboard survey. The estimates are broken down by core and relation to sill depth (see legend). Dark grey bars represent deep cores that were not completely bracketed by observations (Fig. 2). The error bars were determined from the combined instrument and processing uncertainties (see the methods section for details). b) Mean volume transport with respect to temperature and salinity properties of both cores from all transects (the red and black boxes in Fig. 2). The grey contours are density. The transport mode of the IFSJ (NIJ) and its standard deviation is marked in grey (black).

RAFOS floats deployed at 600–800 m depth northeast of Iceland in 2013 and 2014[32], and near the Faroe Islands in 2004[33], drifted southeastward along the slope between Iceland and the Faroe Islands. In the latter case the vast majority of the floats deployed on isobaths shallower than 1750 m turned southeastward into the Faroe Shetland Channel. These observations[33], as well as estimates from a simplified dynamical model[34], suggest that deep currents in this region are strongly guided by bathymetry, which supports the results presented here of the IFSJ.

Inferences from shipboard hydrographic time series

To shed more light on the structure of the IFSJ, we analysed a collection of 120 repeat hydrographic transects along section N directly north of the Faroe Islands (Fig. 1), spanning the last 30 years. While the station spacing of 10 nautical miles is too coarse to properly resolve the IFSJ, we considered the isopycnal structure near the upper slope to identify occupations where particularly dense water ($\sigma_\Theta \geq 28.03\,\mathrm{kg\,m^{-3}}$) was present at the bottom of station 4 (referred to as the "elevated isopycnal" state, 38/120 surveys). We note that only the most extreme occurrences of dense water banked up on the slope are captured due to the large distance between stations. As such, more moderate banking of dense water cannot be resolved. The composite mean of the elevated isopycnal state is shown in Fig. 4.

The surface layer consists of warm, salty water of the Faroe Current. Beneath this, the isopycnal tilt reverses, and cold, dense water is banked up against the slope (Fig. 4a–b). This is characteristic of the IFSJ, and the associated composite section of geostrophic velocity relative to the 28.0 $\mathrm{kg\,m^{-3}}$ isopycnal illustrates the bottom-intensified flow near the slope, directed toward the Faroe Shetland Channel (Fig. 4c). The deep current is located between stations 4 and 5, which encompass the isobaths of both cores of the IFSJ farther upstream. (The combination of the steep continental slope and the coarse station spacing along section N makes it impossible to resolve separate IFSJ cores.)

We estimated the IFSJ volume transport by referencing the composite section of relative geostrophic velocity for the elevated isopycnal state using surface velocities derived from satellite altimetry (see the methods section for details). The transport of overflow water is on the order of 1 Sv, which is consistent with the transport estimated from the high-resolution transects. We note that the uncertainty of this estimate is high because of the wide station spacing and the low spatial resolution of the satellite altimetry data. Nevertheless, the elevated isopycnal state qualitatively resembles the structure and properties of the IFSJ farther upstream. Such elevated isopycnal sections capturing the most extreme banking of dense water were identified in most years and every season, while a finer station spacing would likely also resolve more moderate banking.

Vertical structure and variability from moored measurements

To investigate the vertical structure and variability of the IFSJ, we analysed moored records of direct current velocities at section N. From June 2017 to May 2018, two moorings were deployed at depths of 960 m and 1210 m (Fig. 4c). These were shoreward and seaward, respectively, of the deep IFSJ core (1100 m) seen in the high-resolution shipboard data farther upstream. A combined mean along-stream velocity profile constructed from the two moorings reveals bottom-intensified flow directed toward the FBC (Fig. 5a). The structure and magnitude of the flow is consistent with the IFSJ in the upstream sections (Fig. 2). The mean velocity in the strongest part of the current (below the dashed line in Fig. 5a) was 6.6 $\mathrm{cm\,s^{-1}}$ (Fig. 1b). This is likely an underestimate due to sidelobe reflections from the bottom (see the

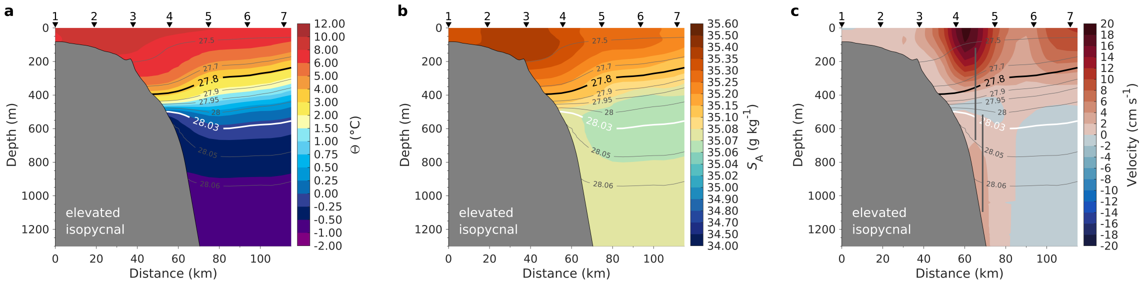

Figure 4: Composite of a subset of vertical sections north of the Faroe Islands. Mean temperature (a), salinity (b), and relative geostrophic velocity (c) for the elevated isopycnal state (see text for details). The $28.03\,\mathrm{kg\,m^{-3}}$ isopycnal used to identify this subset of sections is marked in white, and the $27.8\,\mathrm{kg\,m^{-3}}$ isopycnal, which defines the top of the overflow layer, is the thick black contour. Positive velocities are directed eastward toward the Faroe Shetland Channel. The station numbers are indicated along the top. The vertical grey lines in c) mark the locations and depth ranges of direct velocity measurements from moorings (Fig. 5a).

methods section for details). Short, intermittent periods of negative (northwestward) velocities (Fig. 5d) may be due to lateral meandering of the deep IFSJ core. The mean hydrographic properties closest to the mooring from section N match those of the IFSJ's transport mode (Fig. 5b–c). Taken together, there is strong evidence of a bottom-intensified current resembling the IFSJ at section N.

The inshore mooring in Fig. 4c is part of a long time series of velocity measurements designed to monitor the Atlantic Water transport in the surface-intensified Faroe Current. However, as seen in Fig. 5a, its depth range extends sufficiently deep to capture the upper portion of the IFSJ. Encouragingly, the measurements from the overlapping depth range of the inshore and offshore moorings are well correlated ($r = 0.63$). Furthermore, the variability in the strongest part of the IFSJ from the offshore mooring (below the dashed line in Fig. 5a) is reasonably well correlated ($r = 0.59$) with the uppermost portion of the IFSJ from the inshore mooring (570–675 m). As such, measurements from the inshore mooring can be used as a longer-term proxy for the variability in the IFSJ.

We examined a 7-year long subset of the inshore mooring record (2006–2013) when the mooring was deployed at approximately the same bottom depth (956 ± 5 m). To determine the dominant variability of the along-stream velocity, we computed empirical orthogonal functions (EOFs). The two leading modes explain 68 and 26 % of the variance in the currents, respectively (supplementary information, Fig. S3). The first EOF represents a barotropic mode, where the Faroe Current and the IFSJ

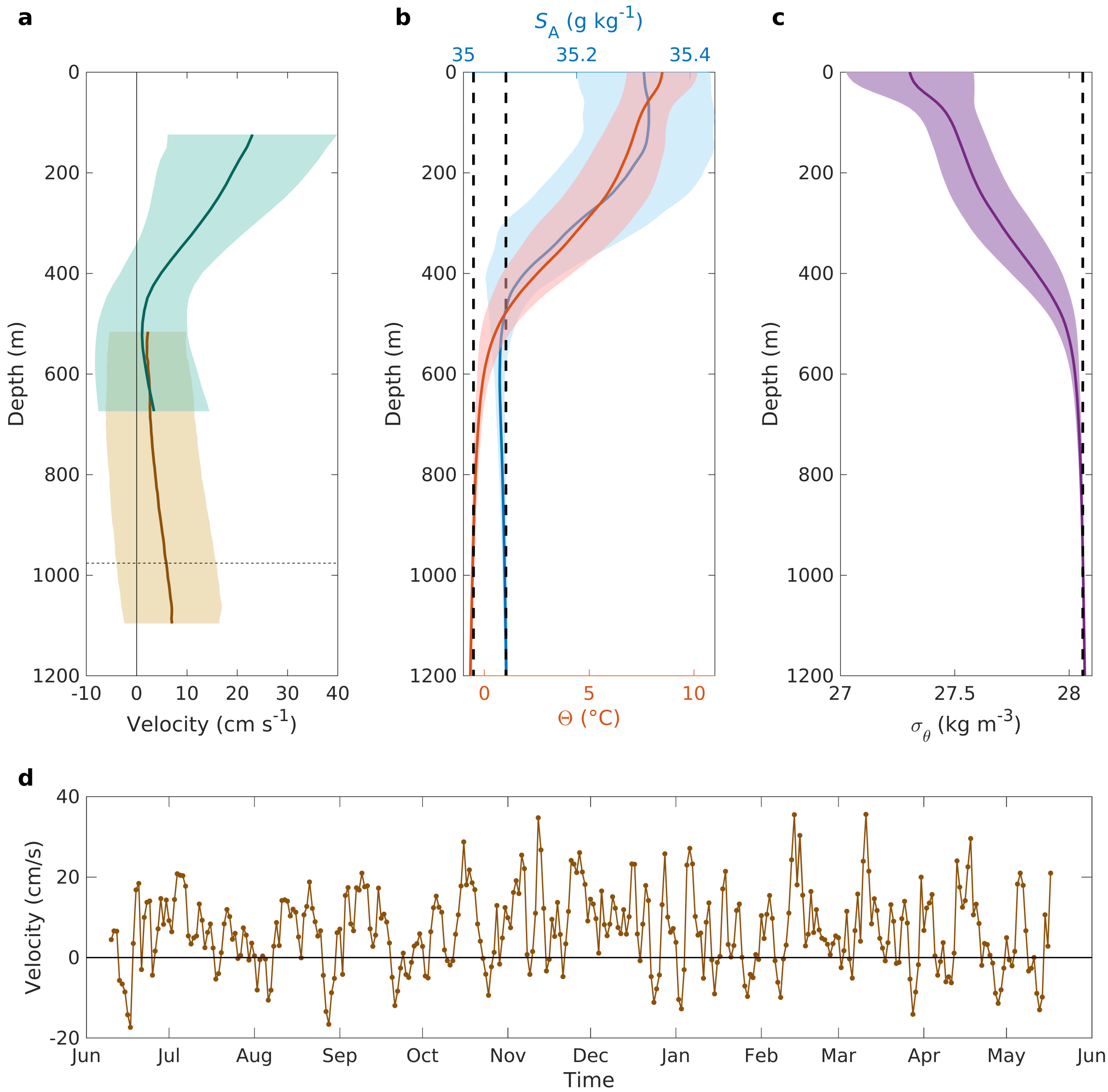

Figure 5: Year-long moored records and hydrographic profiles from section N. a) Mean along-stream velocity profiles from moorings deployed from June 2017 to May 2018 at section N at a bottom depth of 960 m (green) and 1210 m (brown; Fig. 4c). The along-stream direction is defined as 105° clockwise from true north (see methods section for details). The dashed line indicates the upper limit for the velocity depth average in d). b) and c) show mean profiles of temperature (red), salinity (blue), and density (purple) near the offshore mooring from 120 repeat occupations of section N. The properties of the IFSJ transport mode from the high-resolution transects (Fig. 3b) are marked by vertical lines. The shaded areas in a)–c) indicate one standard deviation (the standard error is very small for all profiles). d) Time series of the depth-averaged velocity in the deepest portion of the IFSJ, below the dashed line in a).

are in phase, while the second EOF is a baroclinic mode in which the strength of the Faroe Current and IFSJ vary out of phase.

The principal component of the first EOF mode shows variability on seasonal time scales, while that of the second mode is dominated by variability on a 2–3 week period. We note that the NIJ has no such seasonal signal[6;13;35;36], and, since the IFSJ has similar properties, likely the same source waters, and is located even deeper in the water column, one would not expect a seasonal signal in the IFSJ northeast of Iceland either. While the offshore record at section N is too short to resolve a seasonal cycle, the approximately eastward velocities appear to be enhanced from November to January compared to July and August (Fig. 5d), consistent with the long-term proxy of the IFSJ from the inshore mooring. We surmise that the energetic Faroe Current, which has a pronounced seasonal cycle with maximum eastward flow in winter[37], induces a seasonality in the upper portion of the IFSJ when the currents come into close proximity near section N.

Conclusion

Using four independent observational data sets with different spatial and temporal resolutions, we have provided compelling evidence of a current transporting dense water from northeast Iceland toward the FBC overflow. The current is referred to as the Iceland-Faroe Slope Jet (IFSJ). While previous studies have hinted at the existence of such a flow, the data employed here are extensive and multi-faceted, including the first high-resolution observations of the IFSJ. The current is bottom-intensified and comprises two cores centred on the 750 and 1100 m isobaths along the Iceland-Faroe Ridge. The bulk of the transport is confined to a small range in temperature-salinity space. This transport mode has a density of $\sigma_\Theta = 28.06\,\mathrm{kg\,m^{-3}}$, consistent with the densest waters in the FBC. Long-term repeat shipboard observations support the results of the high-resolution synoptic survey in terms of the presence of dense water banked up along the slope. Direct current measurements corroborate the existence of the IFSJ, and a long-term velocity record demonstrates a link between the variability in the surface-intensified Faroe Current and the uppermost part of the IFSJ. Our measurements suggest that the IFSJ transports approximately 1 Sv of overflow water toward the FBC, which would account for half of the total transport through the passage. As such, the current is a major pathway of dense water to the easternmost overflow ventilating the deep North Atlantic.

Recent studies emphasise the importance of dense water formation in the Nordic Seas in sustaining the lower limb of the AMOC[21;22]. A basic understanding of the origin and the circulation of this dense water mass is thus required for accurate predictions of the future state of the AMOC. Where and how the dense waters are formed is changing[24;38–40], which in turn could affect the composition and the pathways of the dense waters contributing to the overflow across the Greenland-Scotland Ridge. The IFSJ is one of these pathways, and our findings highlight its significance for the overturning circulation and thus the climate system.

Methods

The high-resolution hydrographic/velocity survey, which included eight transects north of Iceland (Fig. 1b), was conducted on R/V *Knorr* in September 2011. The hydrographic data were acquired using a Sea-Bird 911+ conductivity-temperature-depth (CTD) instrument, which was mounted on a rosette with 24 Niskin bottles. Water samples were obtained to calibrate the conductivity sensor, and the final accuracy of the CTD measurements was estimated to be 0.001 °C for temperature, $0.002\,\mathrm{g\,kg^{-1}}$ for salinity, and 0.3 dbar for pressure[13]. Velocities were measured using upward and downward-facing lowered acoustic Doppler current profiler (LADCP) instruments. The velocity measurements were processed using the LADCP Processing Software Package from the Lamont-Doherty Earth Observatory[41;42], and the barotropic tides were removed using an updated version of a regional tidal model[43].

Vertical sections of Conservative Temperature (temperature), Absolute Salinity (salinity), and potential density anomaly (density) were constructed using Laplacian-spline interpolation[44], with a grid spacing of 2 km in the horizontal and 10 m in the vertical. Absolutely referenced geostrophic velocities normal to each transect were calculated as follows: The cross-track ADCP velocities were interpolated onto the 2 km by 10 m regular grid. At each grid point the depth-averaged ADCP velocity was then matched to the depth-averaged relative geostrophic velocity computed from the hydrography. To avoid undue influence from surface and bottom boundary layers, the top and bottom 50 m were excluded from the depth averages. The along-stream direction is defined positive toward the Faroe Shetland Channel. The volume transport of the IFSJ was calculated from the absolutely referenced geostrophic velocity fields. We estimated the uncertainty of the transport from instrument and processing errors scaled by the cross-sectional area of the current. The combined error of the LADCP instrument and the processed velocity data was estimated to be $3\,\mathrm{cm\,s^{-1}}$, while the inaccuracies in the tidal model are $2\,\mathrm{cm\,s^{-1}}$ north of Iceland[5]. The total uncertainty, determined as the root-sum-square of the instrument/processing and tidal model errors, is $3.6\,\mathrm{cm\,s^{-1}}$.

The seven hydrographic stations from the standard monitoring section N north of the Faroe Islands along 6.083 °W (Fig. 1b) are spaced 10 nautical miles apart and were typically occupied three to four times per year between 1987 and 2018. The accuracies of the temperature and salinity measurements are better than 0.001 °C and $0.005\,\mathrm{g\,kg^{-1}}$ from 1997 onwards[37]. Laplacian-spline interpolation was used to construct vertical sections of temperature and salinity, with a grid spacing of 5 km by 10 m. The wide station spacing and steep slope between stations 4 and 5 led to a large “bottom triangle”. This was filled using measurements from the bottom of station 4 prior to interpolation, which helped to conserve the structure of the dense water banked up on the slope. Gridded sections of relative geostrophic velocities referenced to the $28.0\,\mathrm{kg\,m^{-3}}$ isopycnal were constructed from the hydrographic data as above.

We identified sections with the $28.03\,\mathrm{kg\,m^{-3}}$ isopycnal present at depth at station 4 (the “elevated isopycnal” state, 38/120 surveys). Absolute geostrophic velocities at section N were computed using satellite altimetry to reference the relative geostrophic velocities. The transport was estimated by integrating the flow between stations 4 and 5, the bottom, and the $27.8\,\mathrm{kg\,m^{-3}}$ isopycnal which delimits the overflow water. The satellite altimetry data are reprocessed, daily averages of sea level anomaly on a global 0.25 ° by 0.25 ° grid from 1993 to present, compiled from all altimeter missions. The product, previously distributed by Aviso+, can be accessed at E.U. Copernicus Marine Service Information (`http://marine.copernicus.eu/`). We chose data from six grid points near section N for the days coinciding with the hydrographic surveys. Instead of using the mean dynamic topography, which relies on a geoid that is too smooth north of the Faroe Islands, we applied calibration coefficients inferred from direct current measurements from moorings at section N to the satellite altimetry data[37].

We used one year (June 2017 to May 2018) of current measurements from ADCPs on section N at 62.95 °N and 62.92 °N (separated by 3.1 km). The moorings were located at bottom depths of 1210 m and 960 m and measured current speed and direction in ranges of approximately 515–1185 m and 125–675 m, respectively. Daily averages were computed from the velocity time series, which originally were recorded every 20 minutes, after removing the tidal components. The velocities were rotated to align with the direction of the mean flow of the strongest part of the IFSJ below 975 m, which is 105° clockwise from true north.

The velocity measurements of the bottom-mounted ADCP at the offshore mooring are affected by interference from sidelobe reflection. This typically occurs in the lowest 200–300 m, and results in a strong artificial velocity bias toward zero[45;46]. We selected daily profiles with a depth-intensified structure (66 % of all profiles for a velocity maximum above $4\,\mathrm{cm\,s^{-1}}$; the results are not very sensitive to this choice). For each of these profiles we identified the depth of the velocity maximum (1065 m on average) and the depth range of its 90th percentile. The upper value of this range (975 m) is taken to be the limit of the strongest part of the IFSJ. The number of ADCP velocity bins below the lower value of the range follows an exponential distribution (bins near the bottom are most often affected); the cut-off was set to the depth of the 90th percentile of this distribution (1096 m). Measurements of all profiles below this threshold were disregarded. The limit is a compromise between removing too many measurements and keeping profiles that underestimate the true velocity at depth due to the sidelobe interference.

From the long time series of the inshore mooring at section N, we used a 7-year long record (2006–2013) when the mooring was deployed at approximately the same bottom depth of 956 ± 5 m, measuring velocities between 120 and 670 m depth. A lowpass filter of 36 hours was applied to the velocity time series, originally recorded every 20 min, before daily averages were computed. The velocity was rotated to align with the direction of the mean flow of the uppermost part of the IFSJ below 570 m (where the depth-intensification begins) for this time period, which is 98° clockwise from true north. To determine the dominant variability of the velocity, we computed empirical orthogonal functions (EOFs). Before decomposing the velocity time series, we linearly interpolated the gaps of two to four weeks every summer when the mooring was serviced. Different interpolation methods gave quantitatively similar results in the EOF analysis.

Acknowledgements

Support for this work was provided by the Bergen Research Foundation Grant BFS2016REK01 (S.S. and K.V.), the U.S. National Science Foundation Grants OCE-1558742 and OCE-1259618 (R.S.P.), the Danish Ministry of Climate, Energy and Utilities (K.M.H.L., H.H., and B.H.), and the European Union's Horizon 2020 research and innovation programme under grant agreement 727852 (Blue-Action) (K.M.H.L., H.H., and B.H.).

Data availability

The high-resolution hydrographic/velocity data, obtained by the Woods Hole Oceanographic Institution, are available at `http://kogur.whoi.edu/php/index.html#publications`. The hydrographic repeat transects and velocity measurements from the moorings at section N acquired by the Faroe Marine Research Institute are available at `www.envofar.fo`. The gridded satellite altimetry product can be accessed at E.U. Copernicus Marine Service Information (`http://marine.copernicus.eu/`).

Author contributions

R.S.P. led the cruise on R/V *Knorr* and supplied the initial idea for this study. S.S., R.S.P., and K.V. analysed the data and wrote the paper. B.H. and K.M.H.L. led most of the R/V *Magnus Heinason* cruises that provided the hydrographic and velocity data at section N. All authors contributed ideas, interpreted the results, and clarified the implications.

Competing interests

The authors declare no competing financial interests.

References

[1] Årthun, M., Kolstad, E. W., Eldevik, T. & Keenlyside, N. S. Time Scales and Sources of European Temperature Variability. *Geophysical Research Letters* **45**, 3597–3604 (2018).

[2] Eldevik, T. *et al.* A brief history of climate – the northern seas from the Last Glacial Maximum to global warming. *Quaternary Science Reviews* **106**, 225–246 (2014).

[3] Dickson, R. R. & Brown, J. The production of North Atlantic Deep Water: Sources, rates, and pathways. *Journal of Geophysical Research: Oceans* **99**, 12319–12341 (1994).

[4] Swift, J. H. & Aagaard, K. Seasonal transitions and water mass formation in the Iceland and Greenland seas. *Deep Sea Research* **28A**, 1107–1129 (1981).

[5] Våge, K. *et al.* Significant role of the North Icelandic Jet in the formation of Denmark Strait overflow water. *Nature Geoscience* **4**, 723–727 (2011).

[6] Harden, B. *et al.* Upstream sources of the Denmark Strait Overflow: Observations from a high-resolution mooring array. *Deep-Sea Research Part I: Oceanographic Research Papers* **112**, 94–112 (2016).

[7] Mastropole, D. *et al.* On the hydrography of Denmark Strait. *Journal of Geophysical Research: Oceans* **122**, 306–321 (2017).

[8] Spall, M. A. *et al.* Frontogenesis and Variability in Denmark Strait and Its Influence on Overflow Water. *Journal of Physical Oceanography* **49**, 1889–1904 (2019).

[9] Moritz, M., Jochumsen, K., North, R. P., Quadfasel, D. & Valdimarsson, H. Mesoscale Eddies observed at the Denmark Strait sill. *Journal of Geophysical Research: Oceans* 1–33 (2019).

[10] Østerhus, S. *et al.* Arctic Mediterranean exchanges: A consistent volume budget and trends in transports from two decades of observations. *Ocean Science* **15**, 379–399 (2019).

[11] Våge, K. *et al.* Revised circulation scheme north of the Denmark Strait. *Deep-Sea Research Part I: Oceanographic Research Papers* **79**, 20–39 (2013).

[12] Jónsson, S. & Valdimarsson, H. A new path for the Denmark Strait overflow water from the Iceland Sea to Denmark Strait. *Geophysical Research Letters* **31**, L03305 (2004).

[13] Semper, S. *et al.* The emergence of the North Icelandic Jet and its evolution from northeast Iceland to Denmark Strait. *Journal of Physical Oceanography* **49**, 2499–2521 (2019).

[14] Hansen, B. & Østerhus, S. North Atlantic-Nordic Seas exchanges. *Progress in Oceanography* **45**, 109–208 (2000).

[15] Fogelqvist, E. *et al.* Greenland-Scotland overflow studied by hydro-chemical multivariate analysis. *Deep-Sea Research Part I: Oceanographic Research Papers* **50**, 73–102 (2003).

[16] Mauritzen, C., Price, J., Sanford, T. & Torres, D. Circulation and mixing in the Faroese Channels. *Deep-Sea Research Part I: Oceanographic Research Papers* **52**, 883–913 (2005).

[17] Beaird, N. L., Rhines, P. B. & Eriksen, C. C. Overflow Waters at the Iceland-Faroe Ridge Observed in Multiyear Seaglider Surveys. *Journal of Physical Oceanography* **43**, 2334–2351 (2013).

[18] Hansen, B., Larsen, K. M. H., Hátún, H. & Østerhus, S. A stable Faroe Bank Channel overflow 1995-2015. *Ocean Science* **12**, 1205–1220 (2016).

[19] Jeansson, E., Olsen, A. & Jutterström, S. Arctic Intermediate Water in the Nordic Seas, 1991-2009. *Deep Sea Research Part I: Oceanographic Research Papers* **128**, 82–97 (2017).

[20] Turrell, W. R., Slesser, G., Adams, R. D., Payne, R. & Gillibrand, P. A. Decadal variability in the composition of Faroe Shetland Channel bottom water. *Deep-Sea Research Part I: Oceanographic Research Papers* **46**, 1–25 (1999).

[21] Chafik, L. & Rossby, T. Volume, Heat, and Freshwater Divergences in the Subpolar North Atlantic Suggest the Nordic Seas as Key to the State of the Meridional Overturning Circulation. *Geophysical Research Letters* **46**, 4799–4808 (2019).

[22] Lozier, M. S. *et al.* A sea change in our view of overturning in the subpolar North Atlantic. *Science* **363**, 516–521 (2019).

[23] Brakstad, A. *et al.* Historical hydrographic measurements in the Nordic Seas, data set under registration.

[24] Huang, J. *et al.* Sources and upstream pathways of the densest overflow in the Nordic Seas, submitted.

[25] Amante, C. & Eakins, B. ETOPO1 1 arc-minute global relief model: Procedures, data sources, and analysis. *NOAA Technical Memorandum NESDIS*

NGDC-24 25 (2009). URL https://www.ngdc.noaa.gov/mgg/global/relief/ETOPO1/docs/ETOPO1.pdf.

[26] Hansen, B. & Østerhus, S. Faroe Bank Channel overflow 1995-2005. *Progress in Oceanography* **75**, 817–856 (2007).

[27] Brakstad, A., Våge, K., Håvik, L. & Moore, G. W. K. Water mass transformation in the Greenland Sea during the period 1986-2016. *Journal of Physical Oceanography* **49**, 121–141 (2019).

[28] Nikolopoulos, A., Borenäs, K., Hietala, R. & Lundberg, P. Hydraulic estimates of Denmark Strait overflow. *Journal of Geophysical Research* **108** (2003).

[29] Girton, J. B., Pratt, L. J., Sutherland, D. A. & Price, J. F. Is the Faroe Bank Channel Overflow Hydraulically Controlled? *Journal of Physical Oceanography* **36**, 75–89 (2006).

[30] Hopkins, T. S., Baldasserini, G., Minnett, P., Povero, P. & Zanasca, P. Icelandic Current Experiment. GIN SEA Cruise 88 - Data Report. Hydrography and Circulation. Tech. Rep. SM-260, Saclant Undersea Research Centre (1992).

[31] Yang, J. & Pratt, L. J. Some Dynamical Constraints on Upstream Pathways of the Denmark Strait Overflow. *Journal of Physical Oceanography* **44**, 3033–3053 (2014).

[32] de Jong, M. F., Søiland, H., Bower, A. S. & Furey, H. H. The subsurface circulation of the Iceland Sea observed with RAFOS floats. *Deep-Sea Research Part I: Oceanographic Research Papers* **141**, 1–10 (2018).

[33] Søiland, H., Prater, M. D. & Rossby, T. Rigid topographic control of currents in the Nordic Seas. *Geophysical Research Letters* **35** (2008).

[34] Nøst, O. A. & Isachsen, P. E. The large-scale time-mean ocean circulation in the Nordic Seas and Arctic Ocean estimated from simplified dynamics. *Journal of Marine Research* **61**, 175–210 (2003).

[35] Behrens, E., Våge, K., Harden, B., Biastoch, A. & Böning, C. W. Composition and variability of the Denmark Strait Overflow Water in a high-resolution numerical model hindcast simulation. *Journal of Geophysical Research: Oceans* **122**, 2830–2846 (2017).

[36] Huang, J. *et al.* Structure and Variability of the North Icelandic Jet From Two Years of Mooring Data. *Journal of Geophysical Research: Oceans* **124** (2019).

[37] Hansen, B. *et al.* Transport of volume, heat, and salt towards the Arctic in the Faroe Current 1993-2013. *Ocean Science* **11**, 743–757 (2015).

[38] Lique, C. & Thomas, M. D. Latitudinal shift of the Atlantic Meridional Overturning Circulation source regions under a warming climate. *Nature Climate Change* **8**, 1013–1020 (2018).

[39] Våge, K., Papritz, L., Håvik, L., Spall, M. A. & Moore, G. W. K. Ocean convection linked to the recent ice edge retreat along east Greenland. *Nature Communications* **9** (2018).

[40] Moore, G. W. K., Våge, K., Pickart, R. S. & Renfrew, I. Decreasing intensity of open-ocean convection in the Greenland and Iceland seas. *Nature Climate Change* **5**, 877–882 (2015).

[41] Thurnherr, A. M. A Practical Assessment of the Errors Associated with Full-Depth LADCP profiles Obtained Using Teledyne RDI Workhorse Acoustic Doppler Current Profilers. *Journal of Atmospheric and Oceanic Technology* **27**, 1215–1227 (2010).

[42] Thurnherr, A. M. How To Process LADCP Data With the LDEO Software (2018). URL `ftp://ftp.ldeo.columbia.edu/pub/LADCP/UserManuals/LDEO{_}IX.pdf`.

[43] Egbert, G. D. & Erofeeva, S. Y. Efficient Inverse Modeling of Barotropic Ocean Tides. *Journal of Atmospheric and Oceanic Technology* **19**, 183–204 (2002).

[44] Pickart, R. S. & Smethie, W. M. Temporal evolution of the deep western boundary current where it enters the sub-tropical domain. *Deep Sea Research Part I: Oceanographic Research Papers* **45**, 1053–1083 (1998).

[45] Jochumsen, K. *et al.* Revised transport estimates of the Denmark Strait overflow. *Journal of Geophysical Research: Oceans* **122**, 3434–3450 (2017).

[46] Hansen, B., Larsen, K. M. H., Kristiansen, R., Mortensen, E. & Østerhus, S. Faroe Bank Channel overflow 2012-2013. Tech. Rep. (2014).

Supplementary information

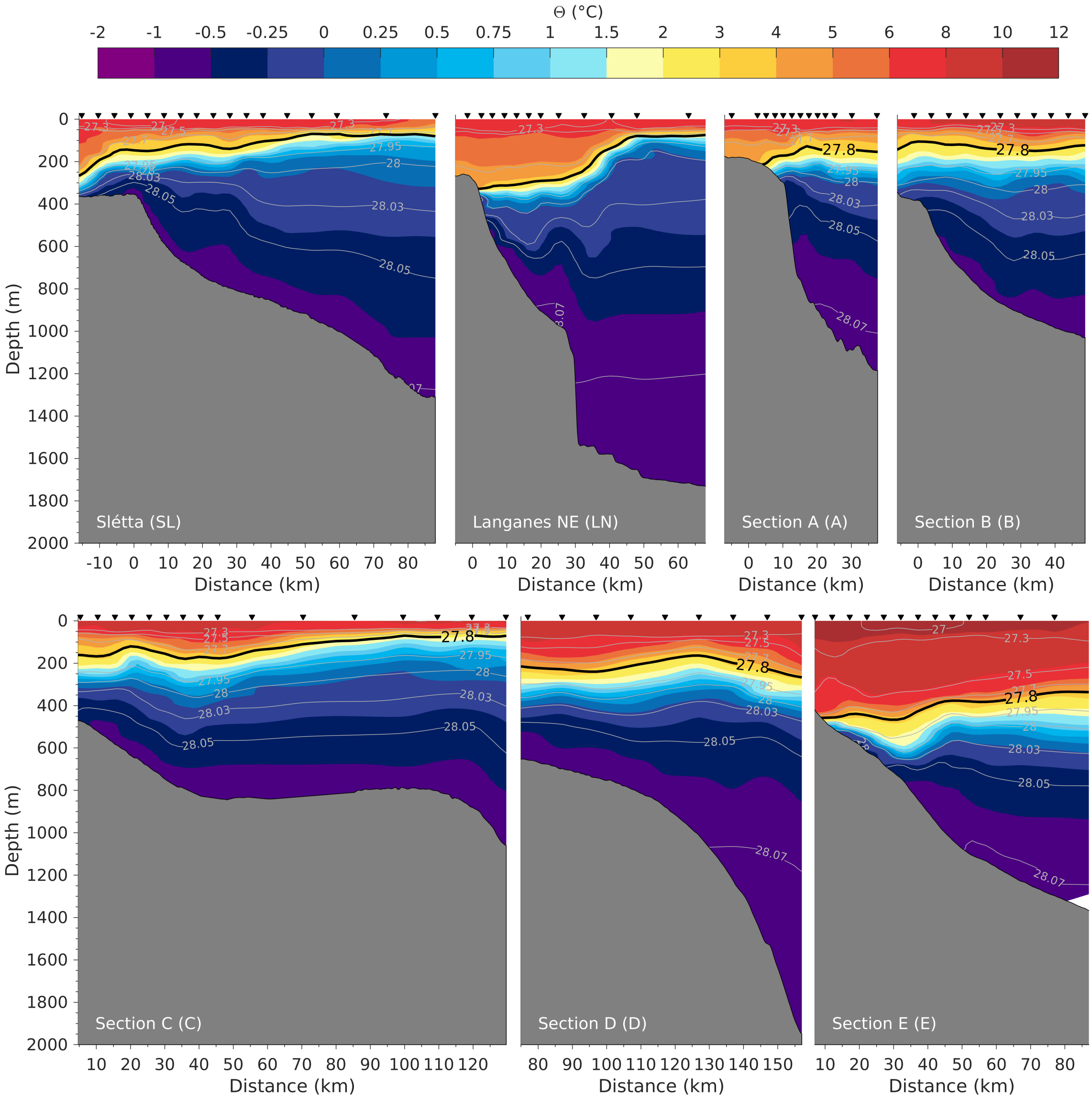

Figure S1: Vertical sections of temperature across the IFSJ. Temperature (colour) and density (thin grey lines) for the yellow segments of the shipboard transects in Fig. 1b. The thick black line is the 27.8 kg m^{-3} isopycnal. The black inverted triangles indicate the locations of the stations. The abbreviated names of the transects are used as labels in Fig. 1. The bathymetry is from the ship's echosounder.

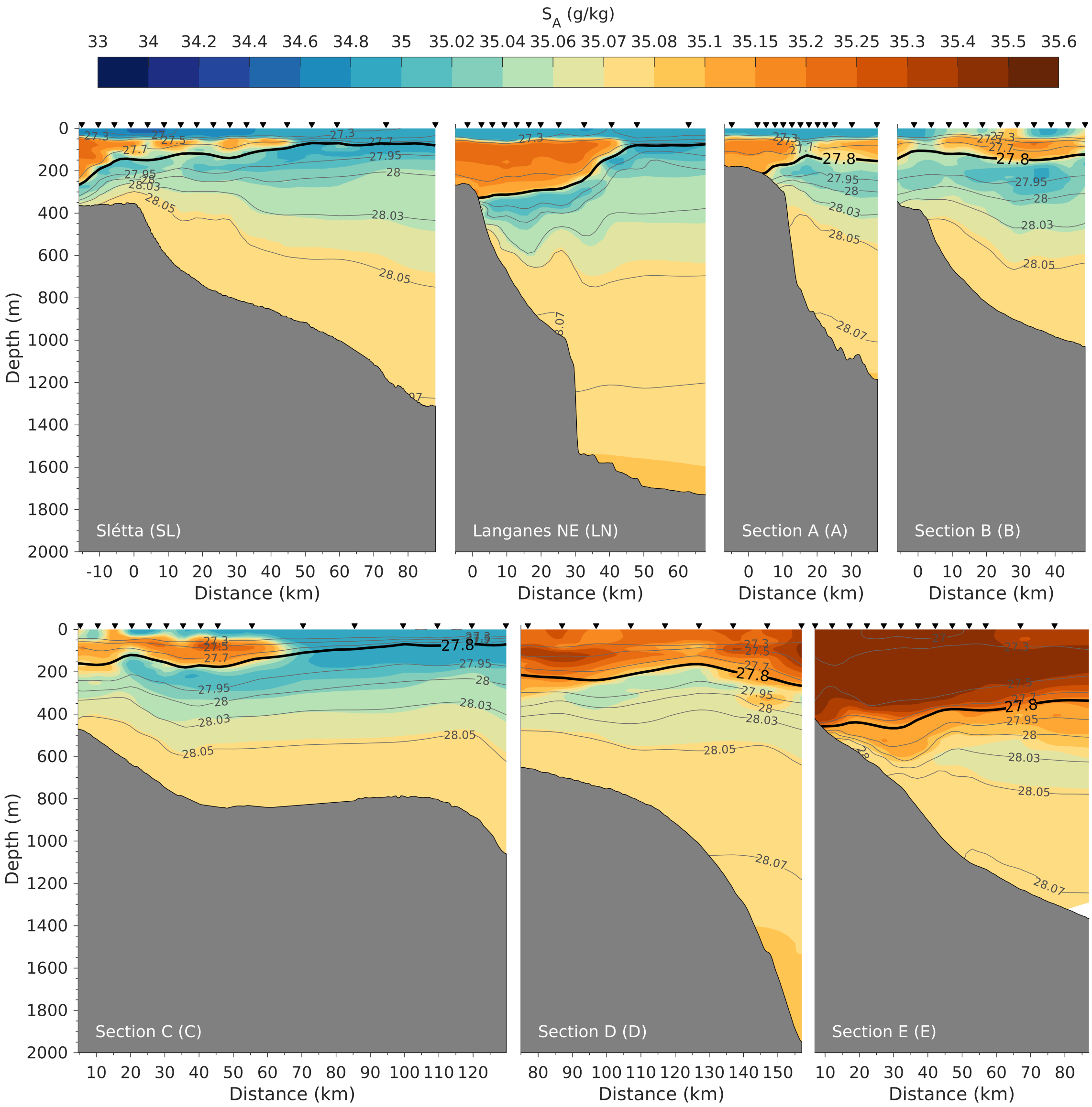

Figure S2: Vertical sections of salinity across the IFSJ. Same as Fig. S1 except for salinity.

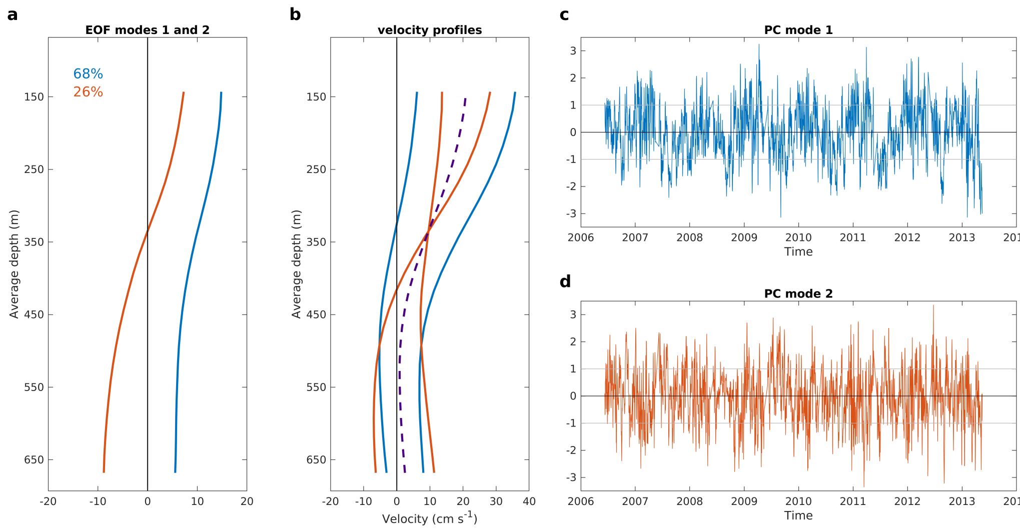

Figure S3: Dominant variability of the along-stream velocity from the inshore moored record at section N (2006–2013). a) Empirical orthogonal function (EOF) modes 1 (blue) and 2 (red), explaining 68 and 26 % of the variance, respectively. b) Mean along-stream velocity profile (purple, dashed line) and velocity profiles (blue: mode 1, red: mode 2) for times when the principal components for mode 1 and 2 are positive and negative one standard deviation. c) and d) Principal component time series for mode 1 (PC1) and mode 2 (PC2). The units are normalised by the standard deviation.